Departmental Papers (ESE)   Department of Electrical & Systems Engineering

October 2007

Optical 'Shorting Wires'

Andrea Alù
University of Pennsylvania, andreaal@seas.upenn.edu

Nader Engheta
University of Pennsylvania, engheta@seas.upenn.edu

Optical 'Shorting Wires'

Abstract

Connecting lumped circuit elements in a conventional circuit is usually accomplished by conducting wires that act as conduits for the conduction currents with negligible potential drops. More challenging, however, is to extend these concepts to optical nanocircuit elements. Here, following our recent development of optical lumped circuit elements, we show how a special class of nanowaveguides formed by a thin core with relatively large (positive or negative) permittivity surrounded by a thin concentric shell with low permittivity may provide the required analogy to 'wires' for optical nano-circuits.

Keywords

Comments

Optical 'Shorting Wires'

Andrea Alù and Nader Engheta

University of Pennsylvania, Department of Electrical and Systems Engineering,
200 South 33rd Street, Philadelphia, PA 19104, U.S.A.
andreaal@ee.upenn.edu, engheta@ee.upenn.edu

http://www.ee.upenn.edu/~engheta/, http://www.ee.upenn.edu/~andreaal/

Abstract: Connecting lumped circuit elements in a conventional circuit is usually accomplished by conducting wires that act as conduits for the conduction currents with negligible potential drops. More challenging, however, is to extend these concepts to optical nanocircuit elements. Here, following our recent development of optical lumped circuit elements, we show how a special class of nanowaveguides formed by a thin core with relatively large (positive or negative) permittivity surrounded by a thin concentric shell with low permittivity may provide the required analogy to 'wires' for optical nano-circuits.

OCIS codes: 999.999 (Nanocircuits); 350.4600 (Optical engineering); 240.6680 (Surface plasmons); 290.5850 (Scattering, particles).

References and links

1.   R. W. Rendell, and D. J. Scalapino, "Surface plasmons confined by microstructures on tunnel junctions," Phys. Rev. B **24**, 3276 (1981).
2.   X. C. Zeng, P. M. Hui, D. J. Bergman, and D. Stroud, "Correlation and clustering in the optical properties of composites: a numerical study," Phys. Rev. B **39**, 13224 (1989).
3.   D. A. Genov, A. K. Sarychev, V. M. Shalaev, and A. Wei, "Resonant field enhancement from metal nanoparticle arrays," Nano Lett. **4**, 153 (2004).
4.   A. I. Csurgay, and W. Porod, "Surface plasmon waves in nanoelectronic circuits," Int. J. Circuit Theory and Applications **32**, 339 (2004).
5.   N. Engheta, A. Salandrino, and A. Alù, "Circuit elements at optical frequencies: nano-inductors, nano-capacitors and nano-resistors," Phys. Rev. Lett. **95**, 095504 (2005).
6.   A. Alù, A. Salandrino, and N. Engheta, "Parallel, series, and intermediate interconnections of optical nanocircuit elements - Part 2: nanocircuit and physical interpretation," submitted to J. Opt. Soc. Am. B, online at: http://arxiv.org/abs/0707.1003.
7.   A. Alù, and N. Engheta, "Optical nano-transmission lines: synthesis of planar left-handed metamaterials in the infrared and visible regimes," J. Opt. Soc. Am. B **23**, 571-583 (2006).
8.   A. Alù, and N. Engheta, "Theory of linear chains of metamaterial/plasmonic particles as sub-diffraction optical nanotransmission lines," Phys. Rev. B **74**, 205436 (2006).
9.   M. G. Silveirinha, A. Alù, J. Li, and N. Engheta, "Nanoinsulators and nanoconnectors for optical nanocircuits," under review, online at: http://arxiv.org/abs/cond-mat/0703600.
10. E. D. Palik, Handbook of Optical Constants of Solids (Academic, San Diego, 1985).
11. S. A. Ramakrishna, J. B. Pendry, M. C. K. Wiltshire, and W. J. Stewart, "Imaging the near field," J. Mod. Opt. **50**, 1419-1430 (2003).
12. CST Studio Suite 2006B, www.cst.com.
13. J. A. Stratton, Electromagnetic Theory (McGraw-Hill, New York, 1941).
14. A. Alù, F. Bilotti, N. Engheta, and L. Vegni, "Theory and simulations of a conformal omni-directional sub-wavelength metamaterial leaky-wave antenna," IEEE Trans. Antennas Propag. **55**, 1698-1708 (2007).
15. A. Alù, M. G. Silveirinha, A. Salandrino, and N. Engheta, "Epsilon-near-zero metamaterials and electromagnetic sources: tailoring the radiation phase pattern," Phys. Rev. B **75**, 155410 (2007).

1. Introduction

Interpreting light interaction with plasmonic nanostructures in terms of circuit models has been considered and discussed in the literature in the past (see, e.g., [1-4]). Recently, we have considered extending the classical circuit theory to nanocircuits at optical frequencies, by exploring the possibility of quantitatively designing nanoparticles to act as individual "lumped" circuit elements with desired lumped impedances in the optical domain [5]. In particular, we have shown that it may be possible to realize lumped nanoinductors, nanocapacitors and nanoresistors by utilizing sub-wavelength nanoparticles with negative-real-part (plasmonic), positive-real-part (non-plasmonic) and imaginary (lossy) permittivity, respectively. In this framework, the role of conduction current density flowing in classic circuits is replaced by the displacement current density $J_d = -i\omega\varepsilon E$ circulating in such a nanocircuit, with ω being the operating radian frequency under an $e^{-i\omega t}$ time convention and ε the local permittivity. While for a single element it has been proven that the classic Kirchhoff laws in the circuit theory are satisfied in this nanocircuit paradigm [5] in terms of the current I defined as the flux integral of J_d across the optical nanoelement and the optical potential V between its two "ends", it is more intricate to envision a complex nanocircuit containing several closely packed nanocircuit elements connected with a special pattern. Even though we have shown that the basic parallel and series combinations of two optical nanoelements are indeed possible by suitably positioning two interconnected particles with respect to the orientation of the external field [6], and that the optical nanotransmission lines may be designed following simple circuit considerations on periodic arrangements of such elements [7-8], the flexibility and possibility of connecting relatively distant optical lumped nanoelements or in connecting insulated nanoparticles that are closely spaced on a nanocircuit board is not as straightforward as in a classic circuit at lower frequencies [9]. This is because at lower frequencies, at which classic circuits rely on the conduction current ($J_c = \sigma E$, with σ being the local conductivity and E the local electric field) circulating across the elements, the background material (i.e., air) or the substrate of a circuit board are naturally very poorly conducting ($\sigma \simeq 0$), and therefore the elements are connected with each other only through the shorting metallic conducting wires attached to their terminals. At high frequencies (infrared and visible), however, the displacement current J_d on which our nanocircuits rely may also flow in the surrounding background materials, in some sense connecting all nanocircuit nanoelements together in an unwanted manner. In this nanocircuit paradigm, in other words, the role of material conductivity is indeed replaced by the local material permittivity ε. It follows, as discussed in [9], that the equivalent of a poorly conducting material in the framework of our optical nanocircuit theory is represented by a relatively low-permittivity (relative ε-near-zero, ENZ) material, for which J_d is close to zero despite the non-zero values of the local electric field. An ENZ material surrounding a lumped nanocircuit element would indeed "insulate" the element from the unwanted coupling with other neighboring elements, at least for what concerns the displacement current flow in it [9]. Analogously, the role of nanoconnectors may be taken, in this nano-circuit analogy, by relatively large permittivity materials (relative ε-very-large, EVL, either positive or negative large permittivity), which may "connect" relatively distant optical nanoelements with a small potential drop, since for a given level of current J_d the corresponding longitudinal electric field, and the consequent voltage drop, are very low across the EVL connector.

Following these heuristic concepts [5-9], the representation of a complex nanocircuit system is getting closer to realization with feasible materials and technology at optical frequencies, i.e., employing naturally available plasmonic, non-plasmonic and/or polaritonic materials. In order to make the picture more complete, however, it may be desirable to envision an optical "shorting wire" that may connect two parts of an optical nanocircuit or two or more nanocircuit elements, in the same manner as classic metallic conducting wires at lower frequencies allow flow of conduction currents with no current leakage and with

negligible voltage drop. Such an optical "shorting wire" should be able: (a) to pass the displacement current flow with essentially no phase delay, without spreading and leaking it around its path, and (b) to sustain the current flow with a sufficiently low optical potential drop across its terminals. In the following, we investigate the possibility of providing these functionalities of an optical wire in the optical nanocircuit domain, exploiting the anomalous properties of EVL and ENZ materials.

We may heuristically envision the optical "shorting wire" as a cylindrical waveguide with deeply subwavelength cross section that is formed by a core with an EVL material surrounded by a thin ENZ shell, which bounds the displacement current flow in the EVL core and does not allow current leakage across it. Here, we verify this prediction by studying this problem analytically and numerically, demonstrating how a displacement current flow with a low optical potential drop and low phase delay may be indeed obtained with such a structure. Since ENZ and EVL materials may exist at infrared/optical frequencies [10] or they may be realized as layered metamaterials [11], realization of such optical nanowaveguides may be envisioned in the optical domains.

2. Theoretical analysis and numerical results

Consider the geometry of Fig. 1(a): a cylindrical core of permittivity ε_{EVL} surrounded by a shell with permittivity ε_{ENZ} and surrounded by a background material with permittivity ε_0. The corresponding radii are, respectively, a_{core} and a_{shell}. All the material permeabilities are assumed to be the same as that of free space μ_0.
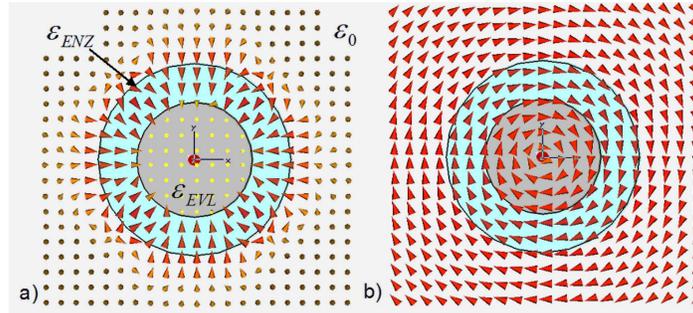

Figure 1 – (Color online) The cross-section of an optical wire composed of an EVL core and an ENZ shell. Electric (a) and magnetic (b) field distribution, snapshot in time, as calculated from full-wave simulations using CST Studio Suite [12] and consistent with Eq. (1) for a nanowire with $a_{core} = 25\,nm$, $a_{shell} = a_{core}/0.6$, $\varepsilon_{ENZ} \simeq (0.01 + i\,0.01)\varepsilon_0$, $\varepsilon_{EVL} \simeq 50\varepsilon_0$ at a background wavelength of $\lambda_0 = 500\,nm$. Arrows are drawn in scale and darker colors correspond to larger field amplitudes.

An azimuthally symmetric TM mode supported by such a waveguide has the following field distributions in each region of space in Fig. 1 [13-14]:

$$\mathbf{H} = \hat{\boldsymbol{\varphi}}\, A\, z_1\left(\sqrt{k^2 - \beta^2}\,\rho\right)e^{i\beta z}$$

$$\mathbf{E} = \hat{\boldsymbol{\rho}}\, A\, \frac{\beta}{\omega\varepsilon}\, z_1\left(\sqrt{k^2 - \beta^2}\,\rho\right)e^{i\beta z} + \qquad (1)$$

$$+ i\,\hat{\mathbf{z}}\, A\, \frac{\sqrt{k^2 - \beta^2}}{\omega\varepsilon}\, z_0\left(\sqrt{k^2 - \beta^2}\,\rho\right)e^{i\beta z}$$

in the corresponding cylindrical reference system of Fig. 1, where β denotes the propagation constant of a guided mode, z_n is the suitable n-th order Bessel function (J_n in the core

region, a linear combination of J_n and Y_n in the shell region and the Hankel function $H_n^{(1)}$ in the background region). Moreover, ε is the local permittivity in the different regions, $k = \omega\sqrt{\varepsilon\mu_0}$ is the local wave number and A a suitable coefficient (different in each region) to match the continuity of the tangential components of fields at the two interfaces. Detailed analytical expression for the field distribution in each region, consistent with Eq. (1), may be found in [14], together with the full-wave dispersion relation for the corresponding guided modes. They have not been repeated here for sake of brevity, but the interested reader may be referred to [14]. Fig. 1 shows an example of these field distributions for a sample geometry.

The general dispersion relation for the modes guided by this structure with arbitrary values for material permittivities is well known [13-14]. Only for $\beta > k_0 = \omega\sqrt{\varepsilon_0\mu_0}$ this dispersion equation admits real solutions, which are the surface waves supported by a core-shell cylinder. In the limit of $|\varepsilon_{EVL}| \gg \varepsilon_0$ and $|\varepsilon_{ENZ}| \ll \varepsilon_0$, together with the deep sub-wavelength cross-sectional dimensions $a_{shell} \ll \lambda_0 = 2\pi/k_0$, the eigen-solutions may be shown to assume the following interesting closed-form expression:

$$\beta^2 = \frac{k_{ENZ}^2}{2\ln a_{shell}/a_{core}}\left[i\pi - 2\frac{J_0\left(k_{EVL}a_{core}\right)}{k_{EVL}a_{core}J_1\left(k_{EVL}a_{core}\right)} - \ln\left(\frac{k_0^2 a_{core}^2}{4}\right) - 2\gamma\right], \qquad (2)$$

where γ is the Euler constant.

This closed-form expression is quite remarkable in its utility to find the propagation constants of guided modes supported by the waveguide of Fig. 1 in the limits of interest here, and it provides many physical insights into its anomalous guidance properties. First of all, it is evident how the values of β are proportional to the wave number in the shell region k_{ENZ}, which tends to zero for low-epsilon shell materials. This is physically expected, due to the low variation of phase in the ENZ material, and is consistent with the findings in [15], regardless of the field excited inside the EVL core. Due to its low value, β is required to be necessarily complex in order to take into account the radiation leakage. In other words, since $\beta < k_0$, the supported modes are leaky-modes, and thus they necessarily radiate in the background region as manifested in the intrinsic complex nature of β given in Eq. (2). (Note some analogies with the structure described in [14]).

The close similarities with a standard shorting conducting wire in a radio-frequency circuit become evident for the traveling modes described by (2): the phase variation along the wire is almost zero (since $\beta \propto k_{ENZ} \simeq 0$) and the electric and magnetic field distributions around it, as depicted in Fig. 1, closely resemble those of a regular conducting wire at radio frequencies. It should be noted that a regular metallic wire also radiates some small energy when a time-varying current flows along its path, and its field distribution is distributed in the background material as described in (1). Usually the radiation losses are negligibly small in classic RF circuits, due to the very small electrical size of RF circuits and the subsequent quasi-static nature of the problem. Even if we are concerned with similar quasi-static distances, Eq. (2) can fully take into account the radiation associated with a displacement current propagating with $\beta \propto k_{ENZ} \simeq 0$ along this optical nanowire, again consistent with its lower frequency counterpart.

If we now consider the limit $\varepsilon_{ENZ} = 0$, we will note that the ENZ shell will act as a perfect magnetic conductor for this TM polarization, reducing the field to zero outside the core and imposing the stringent dispersion relation $J_1\left(\sqrt{k_{EVL}^2 - \beta^2}a_{core}\right) = 0$ on the EVL core radius and/or material. This condition, however, requires a very high positive value of ε_{EVL},

due to the sub-wavelength dimensions of a_{core}, corresponding to a stringent condition for the waveguide design.

Here we consider the scenario that assumes reasonable realistic values for ENZ materials, for which ε_{ENZ}, while still small, is necessarily distinct from zero due to frequency dispersion and the inherent presence of losses. In this case Eq. (2) holds, which may provide more degrees of freedom for the spectrum of possible guided modes supported by this waveguide. Inspecting Eq. (2), we note that for a propagating mode to be supported ($\text{Re}[\beta] \neq 0$) we may just require our geometry to satisfy the following condition:

$$2\frac{J_0\left(k_{EVL}a_{core}\right)}{k_{EVL}a_{core}J_1\left(k_{EVL}a_{core}\right)}+\ln\left(\frac{k_0^2 a_{core}^2}{4}\right)+2\gamma < 0, \tag{3}$$

which imposes some constraints on ε_{EVL} for a fixed dimension of the inner core. (We note how, in this limit, the outer radius of the shell a_{shell} is not crucial in ensuring the guidance properties of Eq. (2), for which condition (3) is sufficient, even though it may play a role in the amplitude of β, appearing in the denominator of Eq. (2)). The imaginary part of β, in this limit and under condition (3), is intrinsically small, since it is proportional to k_{ENZ}. Its value, and the corresponding radiation from the wire, becomes negligible when the left-hand of Eq. (3) becomes sufficiently negative to overcome the term $(i\pi)$ in (2), which happens near the condition $J_1\left(k_{EVL}a_{core}\right)=0$, i.e., when the ENZ shell acts similar to a magnetic boundary.
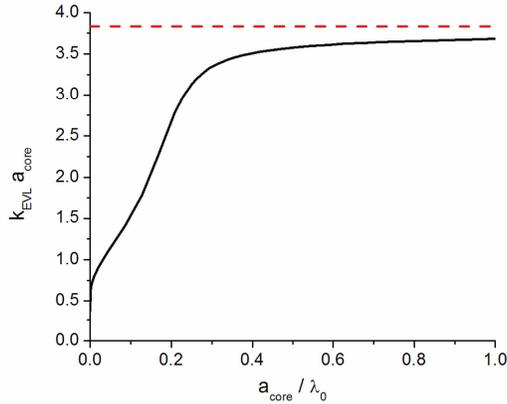

Figure 2 – (Color online) Calculated region of guidance (between the black solid and the red dashed lines) for the waveguide of Fig. 1 in terms of its geometrical parameters.

Figure 2 shows the general region of guidance of the optical nanowire presented here, as predicted by Eq. (2) in the first branch of solutions (those that require the lowest values of ε_{EVL} for a fixed a_{core}/λ_0). The lowest curve (black solid) is the one for which $2\frac{J_0\left(k_{EVL}a_{core}\right)}{k_{EVL}a_{core}J_1\left(k_{EVL}a_{core}\right)}+\ln\left(\frac{k_0^2 a_{core}^2}{4}\right)=-2\gamma$, the highest (red dashed) is the one for which $J_1\left(k_{EVL}a_{core}\right)=0$, which is the upper boundary for the permittivity value of the EVL shell and it coincides with the case when the ENZ shell is replaced by a perfect magnetic boundary. The region included between the two curves guarantees guidance with a complex β with small imaginary part.

As evident from Fig. 2, for small values of a_{core}/λ_0 there is a relatively large range of possible values of ε_{EVL} to have a guided mode in the structure, reasonably smaller than those required in principle if the ENZ shell were replaced by an ideal magnetic boundary. For instance, for an inner core with $a_{core} = \lambda_0/20$, feasible at optical frequencies, a guided mode is supported in the region $13.17\varepsilon_0 < \varepsilon_{EVL} < 148.8\varepsilon_0$. Figure 3, as an example, shows the calculated modal dispersion for a waveguide with $a_{core} = \lambda_0/20$, $a_{shell} = a_{core}/0.8$, varying the material permittivities. Several interesting features are evident in these plots: first of all, consistent with the previous discussion and fairly independent of the value of ε_{ENZ}, the region of guidance is delimited by Eq. (3), which ensures a low imaginary part of β and a fast-wave propagation (low phase variation along the nano-wire) over a broad range of values for ε_{EVL}. It is interesting to note, however, as evident from Fig. 3, that this equation may be satisfied also by negative values of ε_{EVL}, allowing to employ plasmonic materials in the core region, like noble metals and polar dielectrics or semiconductors, widely available in nature at infrared and optical frequencies. The vertical asymptotes in the figure coincide with the roots of the dispersion relation $J_1(k_{EVL}a_{core}) = 0$, that a small waveguide of the same dimensions with magnetic boundaries would support. They separate the different branches for the modes supported by the nanowire. As previously noticed, near these asymptotes at the end of each branch of guided modes $\text{Im}[\beta]$ and the corresponding radiation losses tend to zero.
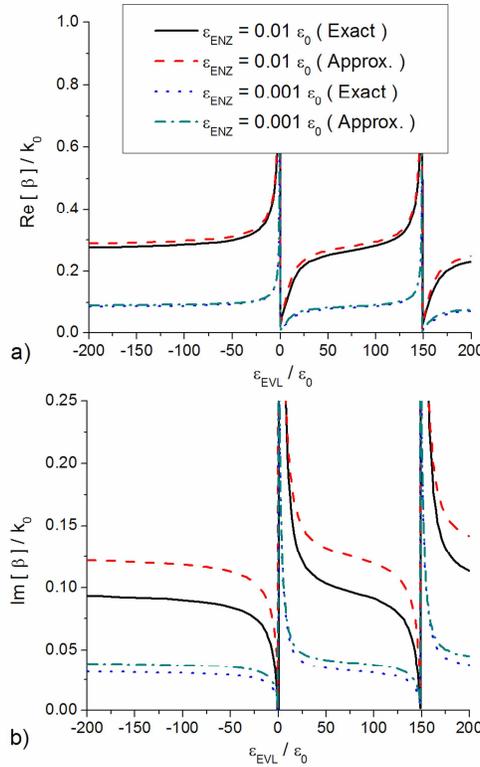

Figure 3 – (Color online) Dispersion of the guided wave number as a function of ε_{EVL} varying ε_{ENZ} for $a_{shell} = a_{core}/0.8$ and $a_{core} = \lambda_0/20$.

For a better understanding of the dispersion properties of the nanowire, the dependence of the wave number in Eq. (2) over the geometrical parameters of a waveguide with $a_{core} = \lambda_0 / 20$ and $a_{shell} = a_{core} / 0.8$ is plotted in Fig. 3 as β versus ε_{EVL} for two different values of ε_{ENZ}. The figure compares the approximate expression (2) with the exact solution of the dispersion equation for the modes supported by the nanowire, showing a good agreement between the exact and approximate lines. The variation of the dispersion curves for a thinner or thicker shell, i.e., varying a_{shell}, is again well described by Eq. (2), which implies a simple scaling of the corresponding value of β as the $\ln a_{shell} / a_{core}$. This implies that a thicker ENZ shell reduces both the phase variation along the wire and the radiation losses, as expectable from the previous physical considerations, due to the better insulation provided by the shell. The same result is obtained by reducing $\left| \varepsilon_{ENZ} \right|$, as seen from the figure, and as consistent with physical considerations. The nanowire operation is indeed appealing, both for positive and negative values of ε_{EVL}, ensuring a relatively broad range of values of permittivities for which the required anomalous guidance may be obtained.

Inspecting the results of Fig. 3(b) concerning the imaginary part of the guided wave number β, it is evident how the damping of such modes due to radiation losses is relatively low, ensuring that in the sub-wavelength scale of an optical nano-circuit these nano-wires may transport the displacement current from one end to the other, with small energy loss (in Fig. 3 we have not considered the presence of material losses, which may enter into play when the nano-wire has a very sub-wavelength cross-section or when the imaginary part of permittivity is relatively high). The results of Fig. 3(b), however, are substantially unchanged when reasonable ohmic losses for optical materials are considered, as we show in the following examples that consider realistic material losses. As an aside, the sign of $\text{Im}\left[\beta\right]$ in Fig. 3 also ensures that the guided modes in that specific example are all forward, independent of the sign of ε_{EVL}. It is proven, more in general, that the sign of ε_{ENZ} is the one to affect directly the direction of propagation of this anomalous mode: backward propagation is obtained when ε_{ENZ} has a negative real part (i.e., before the plasma frequency of the material).
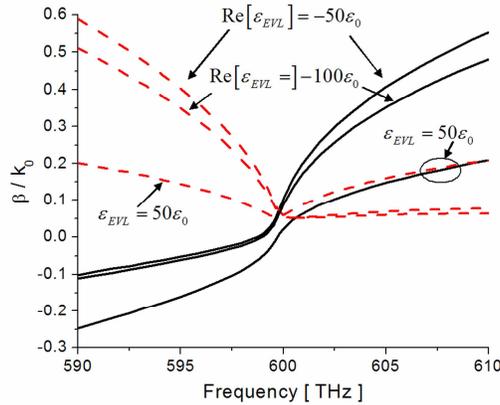

Figure 4 – (Color online) Dispersion of the guided wave number for a nanowire with $a_{shell} = a_{core} / 0.8$ and $a_{core} = 25\,nm$ considering the frequency dispersion of plasmonic materials. Solid black lines refer to the real part of β and dashed red lines to its imaginary part.

This may be seen more in detail in Fig. 4, where the full dispersion of the guided modes for a nano-wire with $a_{shell} = a_{core} / 0.8$ and $a_{core} = 25\,nm$ has been plotted considering the necessary dispersion of the involved plasmonic materials. In this example, the ENZ shell has indeed

been assumed to be plasmonic in nature with a Drude-like dispersion $\varepsilon_{ENZ}(\omega) = \left[1 - \omega_p^2 / \left(\omega(\omega + i\Gamma)\right)\right]\varepsilon_0$, with $\omega_p = 2\pi \cdot 600 THz$ and $\Gamma = 10^{-3}\omega_p$. In this way, we model reasonable dispersion and losses for a plasmonic material at optical frequencies [10]. In the figure three different possibilities are considered for the EVL core material: a positive ε_{EVL}, and two different negative values for the core permittivity. In these latter cases the materials have also been assumed to have a Drude frequency dispersion with corresponding ohmic losses. The values indicated in the figure insets correspond to the permittivity values at $f_p = 600 THz$. In the three cases we obtain nano-wire behavior over a relatively wide range of frequency centered at the plasma frequency of the shell material. The calculated low guided wave number $\mathrm{Re}[\beta]$ and the low damping factor $\mathrm{Im}[\beta]$ ensure the feasibility of the nano-wire for optical nano-circuit applications. It is noted that a positive ε_{EVL} guarantees a wider region of low $\mathrm{Re}[\beta]$, but slightly higher damping factors away from the plasma frequency of the ENZ material. A more negative permittivity for the core material, still in the range of realistic values of permittivity at optical frequencies, as in the example with $\mathrm{Re}[\varepsilon_{EVL}] = -100$, show better performance, as expected. However, reasonable performance over a relatively wide bandwidth is also obtained with a less negative permittivity. It should be noted how, for always positive $\mathrm{Im}[\beta]$, the sign of $\mathrm{Re}[\beta]$ flips together with the sign of $\mathrm{Re}[\varepsilon_{ENZ}]$ at the plasma frequency f_p. This is consistent with the previous discussion on the possibility of forward and backward modes in this regime. The different nature of forward and backward wave propagation above and below f_p, combined with the dispersion properties of the nanowire discussed above, may be responsible for the anomalous slope variation of β versus f in Fig. 4.
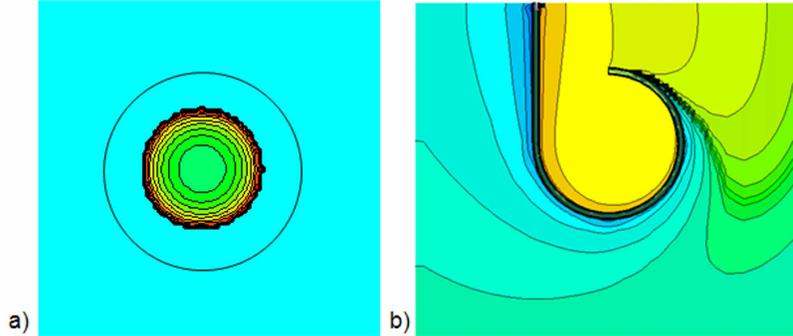

Figure 5 – (Color online) Full-wave simulations (snapshots in time) of: (a) distribution of the optical displacement current density on a transverse cross section of a straight nanowire as in Fig. 1; (b) distribution of the optical magnetic field for a bent nanowire with the geometry of Fig. 1 (the length of the straight section is λ_0 and the radius of curvature of the bend is $\lambda_0/2$). Darker (brighter) colors correspond to higher values.

Figure 5(a) shows the displacement current density $-i\omega\varepsilon_{EVL}E_{core}$ across a cross section of the straight nano-wire of Fig. 1 obtained using numerical simulations [12], and Fig. 5(b) presents the magnetic field distribution for a bent geometry of such a wire (both figures are snapshots in time domain). Since in the RF regime, a metallic wire can still operate as intended, even when it is bent, here we show that this optical "wire" still functions with its interesting properties, when it is bent. Both figures reveal interesting features of such an optical "wire", consistent with the findings described above. In Fig. 5(a) it is evident how the displacement current is all concentrated in the inner core of the nano-wire, similar to a classic shorting

conducting metallic wire at lower frequencies. This is also confirmed by the field distributions reported in Fig. 1, which shows a small longitudinal electric field component in the core, and which resemble those of a classic wire carrying a uniform current. The ENZ shell in this geometry indeed allows confining the displacement current inside the core with a very low optical potential drop (We note that despite the displacement current being high in the core region, the corresponding longitudinal electric field, which contributes to the potential drop along the wire, is very small due to the high value of permittivity of the core material).

A calculation in the quasi-static limit of interest here shows that the impedance per unit length of the nano-wire is given by:

$$Z_{wire} \simeq \left(-i\pi\omega\varepsilon_{EVL}a_1^2 \right)^{-1}. \tag{4}$$

This shows that the impedance of the nanowire is expected to be very small for a sub-wavelength scale. It is interesting to also underline the capacitive/inductive (depending on the sign of ε_{EVL}) behavior of the nanowire, due to the fact that displacement current and voltage are out of phase by 90 degrees. In the example of Fig. 4, the calculated impedance *per unit wavelength* of the designed nanowire is about 77Ω, which ensures a negligible impedance for a sub-wavelength nanocircuit design. It is interesting to notice that this value of impedance per unit wavelength may become much smaller than the one expected from a standard cylindrical waveguide filled by high permittivity materials, another hint of the anomalous guidance properties of the waveguide under analysis.

Fig. 5(b) shows the full-wave simulation of a bent nanowire, demonstrating the striking guidance properties of such an optical 'wire'. It can be seen how the mode is tightly guided around the sub-wavelength waveguide with a very low phase variation along the line. Despite the electrical length of the bent nanowire shown in Fig. 5(b), which is much longer than what would be required in nano-circuit applications, the phase delay along the wire is still negligible and the phase follows the nanowire despite its bend. Also the calculated potential drop along the nanowire is substantially lower than the one expected along a similar electrical length in free-space or along a regular waveguide, since the distribution of longitudinal electric field in the inner region is substantially lower than the transverse electric field in the surrounding free-space (consistent with Fig. 1(a) and the previous discussion).
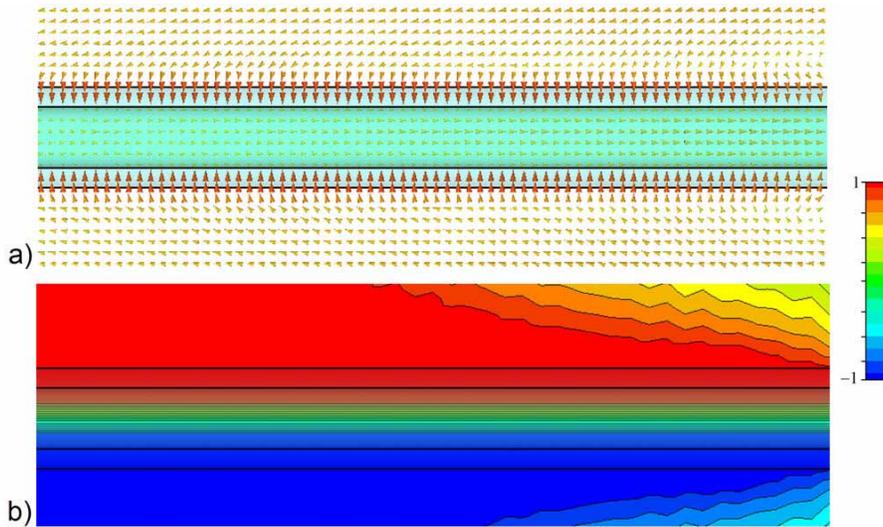

Figure 6 – (Color online) Full-wave simulations (snapshots in time) of (a) electric (tangential to the plane of the figure) and (b) magnetic (orthogonal to the plane of the figure) field distribution for the finite-length straight nanowire of Fig. 5(a). In both scenarios the length of the nanowire section depicted in the figure is about $850\,nm$.

Figure 6 finally confirms this discussion by reporting the electric and magnetic field distributions (snapshots in the time domain) on the longitudinal cross section of the straight nanowire of Fig. 5(a), extracted from numerical full-wave simulations. It is evident how the electric field [Fig. 6(a)] is longitudinally directed inside the nanowire, whereas is transversally directed in the ENZ region. This implies a strong displacement current flowing inside the nanowire and a negligible current flow across the ENZ coating, due to the different values of permittivities in the two regions, consistent with the plots of Fig. 1 and Fig. 5. The orthogonal magnetic field distribution in Fig. 6(b) shows the opposite phase of the magnetic field on the two sides of the nanowire. Both plots, moreover, show uniform phase over a relatively long cross section of the nanowire (over one wavelength in free space) and negligible amplitude decay or radiation losses. Both field distributions, in other words, closely resemble those of a classic shorting wire in a low-frequency circuit and confirm the direct analogy we have drawn in the present manuscript.

3. Conclusions

Here we have reported our findings on how the anomalous guiding properties of an EVL thin cylindrical nanowire surrounded by a thin ENZ plasmonic shell may act as an optical "wire" with interesting potentials in the framework of optical nanocircuit theory and nanoelectronics. The analysis presented here has also derived a closed-form solution for the complex guided wave numbers of this optical wire. Various methods for realization of this optical wire may be forecasted: one way may consist of the use of sub-wavelength stacks of plasmonic and non-plasmonic materials, which, depending on the orientation of the field, may act as effective ENZ or EVL materials (see, e.g., [11]). Another possibility may be by utilizing a relatively high permittivity substrate: since the present analysis has been developed relative to a generic background permittivity ε_0, it is expected that the use of a relatively high-permittivity background may reasonably relax the requirements of a low permittivity for the ENZ shell.